Time-resolved measurements on reflectivity of an ultrafast laser-induced plasma mirror

Yi Cai, Wentao Wang, Changquan Xia, Jiansheng Liu, Li Liu, Cheng Wang, Yi Xu, Yuxin Leng, Ruxin Li, and Zhizhan Xu

Citation: Physics of Plasmas **16**, 103104 (2009); doi: 10.1063/1.3247865
View online: http://dx.doi.org/10.1063/1.3247865
View Table of Contents: http://scitation.aip.org/content/aip/journal/pop/16/10?ver=pdfcov
Published by the AIP Publishing

Time-resolved measurements on reflectivity of an ultrafast laser-induced plasma mirror

Yi Cai, Wentao Wang, Changquan Xia, Jiansheng Liu,[a] Li Liu, Cheng Wang, Yi Xu, Yuxin Leng, Ruxin Li, and Zhizhan Xu[b]
State Key Laboratory of High Field Laser Physics, Shanghai Institute of Optics and Fine Mechanics, Chinese Academy of Sciences, P. O. Box 800-211, Shanghai 201800, China

(Received 12 May 2009; accepted 23 September 2009; published online 20 October 2009)

Using a linearly chirped laser pulse to irradiate antireflection coated targets, the time-varying reflectivity of a plasma mirror (PM) has been measured at various laser intensities from 10^{12} to 10^{17} W/cm^2. The onset of plasma generation as well as the formation process of a PM with the highest reflectivity has been observed. The rise time of the PM's reflectivity reaching up to the maximum varies from 300–500 fs at lower laser intensities but goes up to 900 fs at higher intensity of $>10^{16}$ W/cm^2. This long rise time can be attributed to a slowly rising shoulder of the laser pulse, which will trigger the generation of preplasma well in advance of the laser peak. The detailed measurements on both time-integrated and time-resolved reflectivity of a PM, which is induced by *p*- and *s*-polarized laser pulses, respectively, indicate that an *s*-polarized pulse is favorable to obtain the maximal reflectivity and the best contrast improvement as well. This difference can be attributed to the weaker absorption and a smaller plasma scale length generated for *s*-polarization. © *2009 American Institute of Physics*. [doi:10.1063/1.3247865]

I. INTRODUCTION

With the invention and development of chirped pulse amplification (CPA) technology, tabletop lasers have reached up to an ultrahigh peak power of petawatt and extremely high focused intensity over 10^{21} W/cm^2.[1–3] At such intensity, all matter can be ionized rapidly and the electrons get a relativistic speed, which has led to many new phenomena and opened a new regime of laser-solid interaction.[4]

For a laser pulse with a relativistic intensity, the contrast of peak intensity to prepulse intensity becomes an important parameter that will greatly affect the laser-matter interaction. A conventional CPA femtosecond laser system can only provide a contrast ratio no higher than 10^7. So at the focused spot, the prepulse is very easy to create plasma on the surface of a target before the main pulse arrives. Because of the expansion of the preplasma, the main pulse will not interact on the surface of steep density gradient. This effect has to be avoided in many applications such as ion acceleration[5–7] and high-order harmonic generation from laser-solid interactions.[3,8,9] It is shown recently that a long period prepulse with an intensity as low as 10^8–10^9 W/cm^2 can substantially alter the laser-matter interaction.[10] Various methods have been tested so far to raise the temporal contrast as follows: the methods used inside the laser system, such as cross-polarized-wave,[11,12] polarization rotation in a single-mode fiber[13] and optical parametric CPA;[14] the methods used at the output of the laser, such as frequency doubling[15] and plasma mirrors (PMs).[16–18] The first kind of methods used inside the laser system cannot correct the prepulses caused by uncompensated high-order dispersion in an aberrated compressor. However, PMs and frequency doubling can correct such prepulses. Up to now, the PM technique has been successfully used to improve the temporal contrast ratio for efficiently generating high-order harmonics.[3,8,9] Moreover, the advantage of PMs over other techniques is that they can be cascaded to reach better temporal contrast.[3,9,19]

The PM can be seen as an ultrafast optical switch, because of its very low reflectivity for low-intensity prepulses and high reflectivity for the main pulse. In order to obtain the maximal improvement of contrast ratio, an antireflection (AR) coated glass plate can be selected as an ideal target for the PM. When the intense laser pulses are sent on to the AR-coated target, the low-intensity prepulses are transmitted without damaging the coating, while the main pulse is so intense that its leading edge can ionize the target and generate dense plasma on the target surface by optical field and electronic avalanche ionization. This dense plasma then reflects the remaining part of the incident pulse with very high reflectivity if the plasma does not expand a little and still remains a small density scale length during the interaction. By this way, the contrast between the main pulse and the prepulses can be greatly improved in the reflected pulse. In order to obtain a high-quality PM, quite a few investigations have been made to study the dependence of time-integrated reflectivity of the PM on the laser intensity, pulse duration and the polarization of the laser pulse.[18,20–22] By using a *p*-polarized laser pulse incident upon a SiO_2 target at Brewster's angle, the contrast ratio can be improved by a factor of >625 at intensities of $\sim 10^{16}$ W/cm^2.[17] However, it is found that *s*-polarization is favorable to obtain a higher reflectivity.[22] The temporal shape of the reflected laser pulse and the time-resolved reflectivity of the PM can be diagnosed with a scanning third-order autocorrelation device (TOAD).[19,21,22]

In this work, we focus on the time-resolved measure-

[a]Electronic mail: michaeljs_liu@siom.ac.cn.
[b]Electronic mail: zzxu@mail.shcnc.ac.cn.

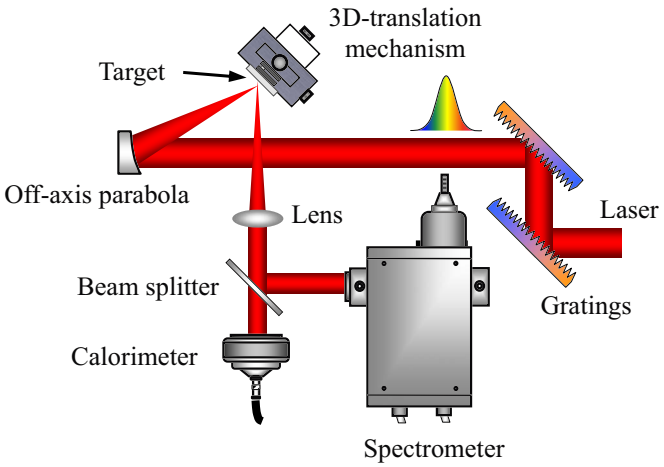

FIG. 1. (Color online) Experimental setup. A calorimeter is placed behind a beam splitter to measure the time-integrated reflectivity of the PM. A spectrometer is used to measure the time-resolved reflectivity of the PM.

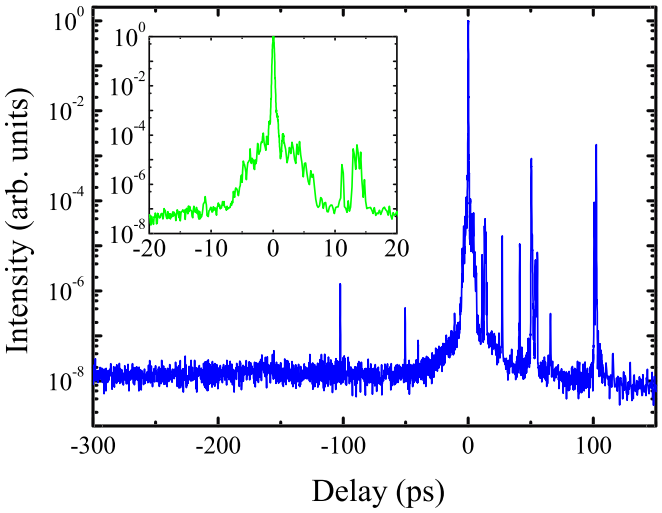

FIG. 2. (Color online) Temporal profile of the laser pulse in a time scale of 300 ps measured by a third-order autocorrelation device. The contrast ratio is 10^8 around 300 ps and 10^5 around 2 ps before the main pulse arrives. Inset: the temporal profile in a time scale of 20 ps.

ments of reflectivity of the PM induced by a subpicosecond laser pulse. Instead of using a TOAD, a time-frequency mapping method is employed here to measure the time-varying reflectivity of the PM during the interaction. The advantage of this method is that a single-shot measurement is needed. We have measured the time-varying reflectivity of the PM at various peak laser intensities from 10^{12} to 10^{17} W/cm^2. The onset of plasma generation and the formation process of the PM have been demonstrated. The rise time of the PM's reflectivity reaching up to the maximum varies from 300–500 fs at lower laser intensities but goes up to 900 fs at higher intensity of $>10^{16}$ W/cm^2. It can be attributed to a slowly rising shoulder of the laser pulse, which will trigger the generation of preplasma well in advance of the laser peak. The detailed measurements on time-integrated reflectivity of the PM for both *p*- and *s*-polarized laser pulses indicate that an *s*-polarized pulse is favorable to obtain the maximal reflectivity and the best contrast improvement as well. A more particular study on the difference between *s*- and *p*-polarization has been done by measuring the time-resolved reflectivity at the intensity of 3×10^{16} W/cm^2. This difference can be attributed to the weaker absorption and a smaller plasma scale length generated for *s*-polarization.

II. EXPERIMENTAL SETUP

The experiments were carried out with a 10 Hz CPA Ti: sapphire laser system which can deliver pulses with 300 mJ energy and 45 fs duration at the central wavelength of 795 nm. The pulse duration can be stretched in the range of 45 fs–1 ps by introducing a slight offset in the distance between the two gratings in the compressor. The experimental arrangement is shown in Fig. 1. A linearly chirped laser beam with a diameter of 50 mm is delivered into the target chamber and focused by an off-axis f/4 parabolic mirror onto an AR-coated glass plate at an incident angle of 32.5°. The focus spot size is measured to be $\sim10\times10$ μm^2. The reflected laser beam is collimated by a lens and then divided by a beam splitter into two beams. One beam is launched into a calorimeter for measuring the time-integrated reflectivity of the PM. The other beam is imaged onto the slit of a spectrometer in order to measure the time-resolved reflectivity of the PM. The target is driven by a three-dimensional translation mechanism to make sure that every shot can interact with a fresh region with the same experimental condition. The polarization of the laser beam can be changed from *s* to *p* by rotating a half wave plate, which is placed before the parabola.

In order to obtain a broad range of peak intensities from 10^{12} to 10^{17} W/cm^2, we adjust the laser intensity on the target in two different ways. First, we adjust the laser energy by rotating a half wave plate placed between two polarizers. Second, the target is moved out of the focus by a *z*-scan controller. By this way, the laser intensity can be greatly decreased owing to the increase of the spot size on the target. The contrast ratio of the incident laser pulse is measured by a TOAD. The third-order correlation is shown in Fig. 2. It can be seen that the contrast ratio is better than 10^7 in a time scale of 300 ps. The peak signals at -100, -50, and -40 ps are artifacts caused by the TOAD. For time-resolved measurement of the PM's reflectivity, we extend the Fourier-limited pulse of 45 fs to a negatively chirped pulse with duration of 500 fs. When the chirped laser pulse irradiates the target, the reflected laser electric field $E_r(t)$ can be expressed as the product of the incident electric field $E_i(t)$ and the time-varying reflectivity $R(t)$ of the PM, $E_r(t)=E_i(t)\times R(t)$. For a linearly chirped laser field, incident electric field $E_i(t)=E_0\exp[-at^2-i(\omega_0 t+bt^2)]$, where E_0 is the amplitude of the incident laser field, a is determined by the pulse duration, $2b$ is the chirp rate, and ω_0 is the central frequency of the laser pulse. If the chirp rate is large enough and the rise time of $R(t)$ is much longer than the Fourier-limited pulse duration (45 fs in our case), the spectra $E_r(\omega)$ of the reflected laser pulse, which is the Fourier transformation of $E_r(t)$, can be given as[23]

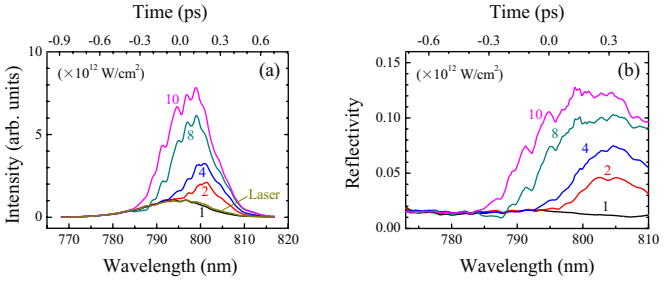

FIG. 3. (Color online) (a) Reflected spectra of 500 fs linearly chirped pulses on an AR-coating plate target for different laser intensities from 1×10^{12} to 1×10^{13} W/cm^2. The intensity is normalized by $I_i^{\text{peak}}R_0$, where I_i^{peak} is the incident peak intensity of the incident laser pulse, and R_0 is the cold reflectivity of AR-coated target. The laser spectrum with a peak intensity of 1 is also shown for comparison with the reflected spectra. (b) Time-resolved reflectivity calculated from (a) by $|R(t)|^2=I_r(\omega)/I_i(\omega)$.

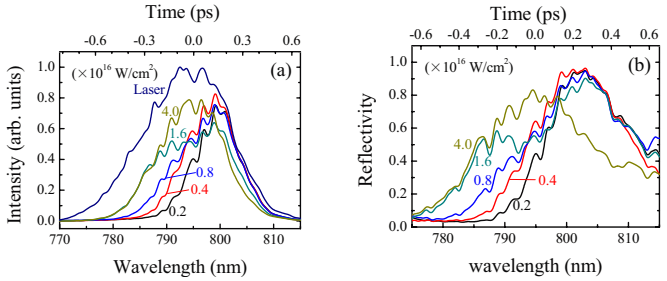

FIG. 4. (Color online) (a) Reflected spectra of 500 fs linearly chirped pulses on an AR-coating plate target, for different laser intensities from 2×10^{15} to 4×10^{16} W/cm^2. The intensity is normalized by the peak intensity of the incident laser pulse. (b) Time-resolved reflectivity calculated from (a) by $|R(t)|^2=I_r(\omega)/I_i(\omega)$.

$$E_r(\omega)=E_i(\omega)\times R\left(\frac{b}{2}\frac{\omega-\omega_0}{a^2+b^2}\right)=E_i(\omega)\times R(t), \tag{1}$$

where $t=(b/2)(\omega-\omega_0/a^2+b^2)$. Therefore, there is a one-to-one mapping between time and frequency. The time-dependent reflectivity $|R(t)|^2$ can be extracted as $|R(t)|^2=I_r(\omega)/I_i(\omega)$. $I_r(\omega)$, and $I_i(\omega)$ are the spectral intensities of reflected and incident laser pulses, respectively. The temporal resolution of this method is $\tau_r=\sqrt{N}\tau_0$ (Ref. 23), where N and τ_0 are the stretching fold and the Fourier-limited pulse duration, respectively. In our experiments, the time resolution is $\tau_r\approx140$ fs. On the other hand, the spectral blueshift caused by the motion of the plasma-vacuum surface toward the incident laser beam might distort the spectrum and affect the measurements if the intense laser drives a very fast motion of the surface. For a laser pulse with duration of 500 fs, the spectral blueshift begins to affect the measurements only when the laser intensity is higher than 2×10^{16} W/cm^2.[21] In addition to measuring the time-integrated reflectivity of the PM, the calorimeter in our experiments can be used to calibrate the spectral intensity recorded by the spectrometer.

III. EXPERIMENTAL RESULTS

Figure 3(a) shows the spectra of the reflected laser pulses we have measured at lower peak intensities from 1×10^{12} to 1×10^{13} W/cm^2, which correspond to the incident fluences from 0.5 to 5 J/cm^2. The spectra are spatially integrated along the slit direction of the spectrometer. The incident laser pulse is negatively chirped to 500 fs from 45 fs and p-polarized. The frequency scale can be converted into a time scale with $\omega=2/b(a^2+b^2)t+\omega_0$. For negatively chirped pulse, the chirp rate b has a minus value. It means that the high frequency component is located at the leading edge of the laser pulse. The spectral intensity shown in Fig. 3(a) has been normalized by the peak intensity I_i^{peak} of the incident laser pulse and the cold reflectivity R_0 of the AR-coated target, i.e., $I_r(\omega)/(I_i^{\text{peak}}R_0)$. The spectrum of the incident laser pulse is also shown in Fig. 3(a). It can be seen that at an intensity of 1×10^{12} W/cm^2, the spectrum of the reflected pulse has a similar profile with that of the incident pulse. While increasing the peak intensity from 2×10^{12} to 1×10^{13} W/cm^2, the profile of reflected spectrum starts to deviate from the incident spectrum. The onset of spectral deviation occurs at longer wavelengths of 795 nm at an intensity of 2×10^{12} W/cm^2, and then shifts to a shorter wavelength of 785 nm at 1×10^{13} W/cm^2. There is a segment of spectrum with shorter wavelengths where the profile remains the same as the incident spectrum. It is attributed to the direct reflection of the AR-coated target without plasma's being generated yet.

Figure 3(b) shows the time-dependent reflectivity for different laser intensities. It is calculated from Fig. 3(a) by $|R(t)|^2=I_r(\omega)/I_i(\omega)$. In our experiments, the reflectivity of the AR-coated target is 1.5%. The evolutions of the time-dependent reflectivity at different laser intensities indicate the following. (1) The threshold laser intensity to generate plasma on the surface of the AR-coated target is above 1×10^{12} W/cm^2 for a 500 fs incident pulse. (2) As the incident intensity increases from 2×10^{12} to 1×10^{13} W/cm^2, the maximal reflectivity of the PM increases from 4.5% to 12.5%. However, at the leading edge of the laser pulse where the laser intensity is lower than 1×10^{12} W/cm^2, the reflectivity remains the same as R_0 (1.5%). (3) The time-dependent reflectivity does not obtain the maximal value at the peak intensity (instant $t=0$), but continues to increase at the tailing edge of the laser pulse ($t>0$). It means that the plasma is produced not mainly by multiphoton ionization but by electron avalanche ionization mechanism.

Figure 4(a) shows the spectra of the reflected laser pulses we have measured at higher peak intensities from 2×10^{15} to 4×10^{16} W/cm^2. The spectral intensity here is normalized by the peak intensity of the incident laser pulse, i.e., $I_r(\omega)/I_i^{\text{peak}}$. The calculated time-dependent reflectivities for different laser intensities are shown in Fig. 4(b). It can be seen that the maximal reflectivity of the PM can be as high as 90% although the time-integrated reflectivity is just around 50%–60%. Shown in Fig. 5 is the rise time of the reflectivity as a function of laser intensity, which is calculated from the measured data, as shown in Figs. 3(b) and 4(b). The rise time here is defined as the time interval from the onset of reflectivity's rising edge to the maximum. It can be seen that as the laser intensity increases from 2×10^{12} to 4×10^{15} W/cm^2, the rise time increases from 300 to 500 fs. As shown in Figs. 3 and 4, the rising edge of the reflectivity was observed to move to earlier times by increasing the laser

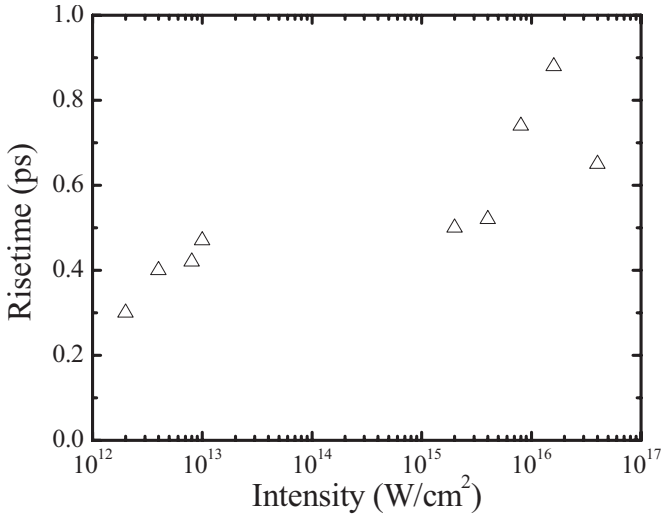

FIG. 5. The rise time of the reflectivity as a function of laser intensity, which is calculated from the measured data, as shown in Figs. 3(b) and 4(b).

intensity. The maximum reflectivity was also observed to move to earlier times from 300 to 100 fs after the laser peak passed. However, there is a fluctuation in the rise time from 600 to 900 fs when the laser intensity is higher than 4×10^{15} W/cm^2. The measured time scale (300–500 fs) of rise time at lower laser intensities in our experiment is in agreement with those measured by Dromey *et al.*[21] and Nomura *et al.*,[22] but longer than the rise time (150 fs) reported previously by von der Linde *et al.*[24,25] The cause may be that a longer pulse duration of 500 fs is employed here. On the other hand, the laser pulse in our experiment is quite imperfect to begin with and has a fairly slow rise and a big shoulder within 5 ps, as shown in Fig. 2. This slowly rising shoulder will have an intensity of higher than 10^{12} W/cm^2 and trigger the generation of plasma well in advance of the peak of the pulse if the peak of laser intensity is higher than

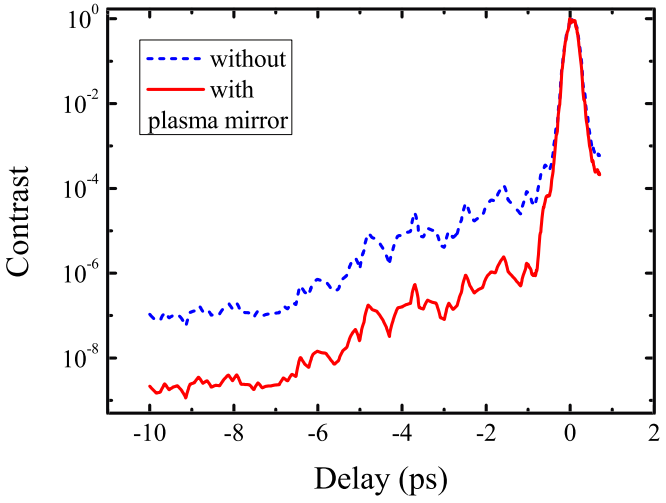

FIG. 6. (Color online) Temporal profile of the reflected laser pulse in comparison with the incident pulse, calculated by the temporal profile of incident laser pulse and the time-varying reflectivity of the PM at 4×10^{16} W/cm^2. Contrast ratio improvement of near two orders of magnitude is seen for the delay time >1 ps before the main pulse arrives.

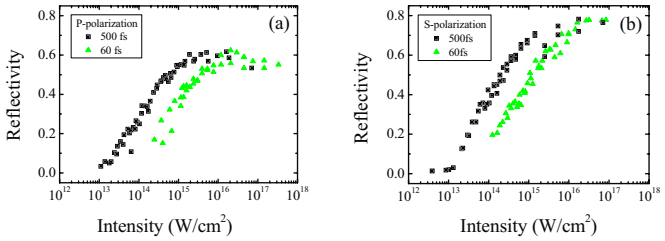

FIG. 7. (Color online) Time-integrated reflectivity for *p*-polarized (a) and *s*-polarized (b) laser pulses as functions of the incident intensity for different pulse durations of 60 and 500 fs.

10^{16} W/cm^2. Thus the rise time of the measured time-resolved reflectivity at higher laser intensity is considerably longer than those measured at lower laser intensities. However, this slowly rising shoulder will be depressed after reflected by the PM. The reflectivity at t=0 can be increased from 40% to 80% as the laser intensity increases from 2×10^{15} to 4×10^{16} W/cm^2. By using the time-varying reflectivity of the PM at 4×10^{16} W/cm^2, the contrast ratio of the reflected pulse can be calculated and is shown in Fig. 6. The contrast ratio has been improved by about two orders of magnitude for the delay time >1 ps before the main pulse arrives, for example, from 10^7 to 10^9 around 10 ps.

Using a calorimeter, we also measured the time-integrated reflectivity as a function of the laser intensity for both *s*- and *p*-polarization. Figure 7(a) shows the time-integrated reflectivity of the PM as a function of laser intensity for *p*-polarized laser pulses with duration of 60 fs and 500 fs, respectively. Shown in Fig. 7(b) is the time-integrated reflectivity as a function of incident intensity for *s*-polarization. For *p*-polarization, the highest reflectivity reaches up to 60%. However it can reach up to 80% for *s*-polarization. For longer pulse duration of 500 fs, the PM can be triggered at lower intensity, but the maximal reflectivity is almost the same as that for 60 fs. It means that the maximal reflectivity is not dependent on the pulse duration in subpicosecond regime. Shown in Figs. 8(a) and 8(b) are the time-integrated reflectivity as a function of incident fluence for *s*- and *p*-polarized pulses with different pulse durations. It can be seen that the evolution of reflectivity is also independent on the pulse duration. For *p*-polarization, the intensity where the maximal reflectivity is reached is around 4×10^{15} W/cm^2 for 500 fs and 2×10^{16} W/cm^2 for 60 fs. However for *s*-polarization, this intensity is around 2×10^{16} W/cm^2. Above this intensity, the reflectivity starts to

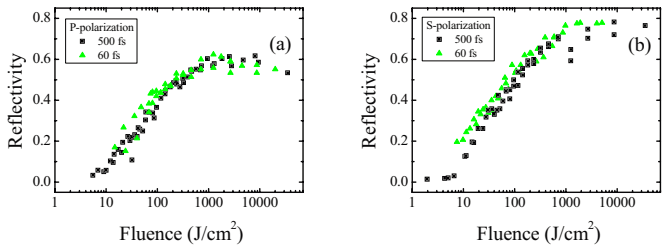

FIG. 8. (Color online) Time-integrated reflectivity for *p*-polarized (a) and *s*-polarized (b) laser pulses as functions of the incident fluence for different pulse durations of 60 and 500 fs, respectively.

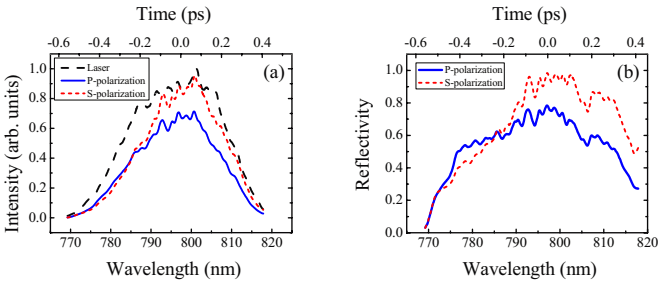

FIG. 9. (Color online) (a) Reflected spectra of 500 fs linearly chirped pulses on an AR-coating plate target at an incident intensity of 3×10^{16} W/cm^2 for *p*- and *s*-polarization, respectively. The intensity is normalized by the peak intensity of the incident laser pulse. (b) Time-resolved reflectivity calculated from (a).

fall. It might be caused by the increased absorption of the laser energy at higher intensity. The difference between *s*- and *p*-polarization can be explained as following: In comparison with *s*-polarization, a *p*-polarized laser pulse has an electric field component in the normal direction of the PM surface, which can induce vacuum heating[26] and resonance absorption.[27] Moreover, at the vicinity of critical density surface, resonance absorption will take away more energy of the incident pulse. On the other hand, electrons will gain more energy and have a higher temperature owing to vacuum heating and resonance absorption. The plasma will expand at a faster speed and have a longer plasma scale length, which is deleterious to obtain a higher reflectivity. Therefore, *s*-polarization is favorable to obtain the maximal reflectivity and the best contrast improvement as well.

The differences of reflectivity between *p*- and *s*-polarization can be investigated in detail from the time-resolved reflectivity. Figure 9(a) shows the reflected spectra of 500 fs linearly chirped pulses on a AR-coating plate target for different polarizations of *p* and *s* at the intensity of 3×10^{16} W/cm^2. The intensity of the reflected spectra is normalized by the peak intensity of the incident laser pulse. Figure 9(b) shows the time-resolved reflectivity calculated from Fig. 9(a). It can be seen that a segment of reflected spectra is coincident at the leading edge. Then the reflectivity for the *p*-polarized pulse rises faster than that for the *s*-polarized pulse. However, around the peak of the incident pulse, the reflectivity for *s*-polarized pulse reach a peak value of 95%, while the maximal reflectivity for *p*-polarized pulse is only 80%. These differences between *p*- and *s*-polarization can help us understand the ionization processes of both polarizations. At the leading edge, the increase of the reflectivity is caused by the optical field ionization, which depends on the intensity of incident pulse, and the reflectivity for both polarizations have the same characteristics. As the incident intensity increases, the *p*-polarized laser pulse with an electric field component in the normal direction will induce vacuum heating and resonance absorption which are helpful for the ionization, and the density of the plasma will increase faster, so the reflectivity should be higher than that of the *s*-polarized laser pulse. However, as the incident intensity continues to increase close to the peak of pulse, the density of the plasma will reach and exceed the critical density, and the stronger absorption for *p*-polarized pulse will take more energy away from the incident laser pulse, which leads to a lower peak reflectivity in comparison with *s*-polarization.

IV. CONCLUSION

In conclusion, we have demonstrated time-resolved measurements on reflectivity of the PM induced by a linearly chirped laser pulse of 500 fs duration. The threshold intensity to generate plasma on the PM surface is around 10^{12} W/cm^2. By increasing the incident intensity to be in the range of 2×10^{15} W/cm^2 to 4×10^{16} W/cm^2, the maximal reflectivity can reach up to as high as 80% although the time-integrated reflectivity is just around 60% for *p*-polarization. The rise time to reach the maximal reflectivity varies from 300 to 500 fs at lower laser intensities but goes up to 900 fs at higher intensity of $>10^{16}$ W/cm^2. It can be attributed to a slowly rising shoulder of the laser pulse, which will trigger the generation of preplasma well in advance of the laser peak. Therefore the intensity of the prepulse in a time scale of picosecond should be lower than 10^{12} W/cm^2 in order to avoid preplasma generation. The maximum time-integrated reflectivity can reach up to 80% for *s*-polarization, while the time-varying reflectivity can obtain the maximum value of 95%. This difference between *s*- and *p*-polarization can be attributed to the vacuum heating and resonance absorption of laser energy for *p*-polarization. It means that an *s*-polarized pulse is favorable to obtain the maximal reflectivity and the best contrast improvement as well. Our experimental results indicate that the evolution of time-integrated reflectivity as a function of incident fluence is independent on the pulse duration in subpicosecond regime.

ACKNOWLEDGMENTS

This work was supported by the Chinese National Natural Science Foundations (Contract No. 10674145), the National Basic Research Program of China (Contract No. 2006CB806000), and Japan-Korea-China Cooperative project on "High Energy Density Sciences for Laser Fusion Energy."

[1] D. Strickland and G. Mourou, Opt. Commun. **56**, 219 (1985).
[2] M. D. Perry, D. Pennington, B. C. Stuart, G. Tietbohl, J. A. Britten, C. Brown, S. Herman, B. Golick, M. Kartz, J. Miller, H. T. Powell, M. Vergino, and V. Yanovsky, Opt. Lett. **24**, 160 (1999).
[3] B. Dromey, M. Zepf, A. Gopal, K. Lancaster, M. S. Wei, K. Krushelnick, M. Tatarakis, N. Vakakis, S. Moustaizis, R. Kodama, M. Tampo, C. Stoeckl, R. Clarke, H. Habara, D. Neely, S. Karsch, and P. Norreys, Nat. Phys. **2**, 456 (2006).
[4] A. Pukhov, Rep. Prog. Phys. **66**, 47 (2003).
[5] R. A. Snavely, M. H. Key, S. P. Hatchett, T. E. Cowan, M. Roth, T. W. Phillips, M. A. Stoyer, E. A. Henry, T. C. Sangster, M. S. Singh, S. C. Wilks, A. MacKinnon, A. Offenberger, D. M. Pennington, K. Yasuike, A. B. Langdon, B. F. Lasinski, J. Johnson, M. D. Perry, and E. M. Campbell, Phys. Rev. Lett. **85**, 2945 (2000).
[6] H. Schwoerer, S. Pfotenhauer, O. Jäckel, K.-U. Amthor, B. Liesfeld, W. Ziegler, R. Sauerbrey, K. W. D. Ledingham, and T. Esirkepov, Nature (London) **439**, 445 (2006).
[7] B. M. Hegelich, B. J. Albright, J. Cobble, K. Flippo, S. Letzring, M. Paffett, H. Ruhl, J. Schreiber, R. K. Schulze, and J. C. Fernández, Nature (London) **439**, 441 (2006).
[8] P. Monot, G. Doumy, S. Dobosz, M. Perdrix, P. D'Oliveira, F. Quéré, F.

Réau, P. Martin, P. Audebert, J.-C. Gauthier, and J.-P. Geindre, Opt. Lett. **29**, 893 (2004).
[9]C. Thaury, F. Quéré, J.-P. Geindre, A. Levy, T. Ceccotti, P. Monot, M. Bougeard, F. Réau, P. d'Oliveira, P. Audebert, R. Marjoribanks, and Ph. Martin, Nat. Phys. **3**, 424 (2007).
[10]K. B. Wharton, C. D. Boley, A. M. Komashko, A. M. Rubenchik, J. Zweiback, J. Crane, G. Hays, T. E. Cowan, and T. Ditmire, Phys. Rev. E **64**, 025401 (2001).
[11]N. Minkovski, S. M. Saltiel, G. I. Petrov, O. Albert, and J. Etchepare, Opt. Lett. **27**, 2025 (2002).
[12]A. Jullien, O. Albert, F. Burgy, G. Hamoniaux, J.-P. Rousseau, J.-P. Chambaret, F. Augé-Rochereau, G. Chériaux, J. Etchepare, N. Minkovski, and S. M. Saltiel, Opt. Lett. **30**, 920 (2005).
[13]J.-L. Tapié and G. Mourou, Opt. Lett. **17**, 136 (1992).
[14]A. Dubietis, G. Jonušauskas, and A. Piskarskas, Opt. Commun. **88**, 437 (1992).
[15]J. Itatani, J. Faure, M. Nantel, G. Mourou, and S. Watanabe, Opt. Commun. **148**, 70 (1998).
[16]H. C. Kapteyn, M. Murnane, A. Skoze, and R. W. Falcone, Opt. Lett. **16**, 490 (1991).
[17]D. M. Gold, Opt. Lett. **19**, 2006 (1994).
[18]G. Doumy, F. Quéré, O. Gobert, M. Perdrix, Ph. Martin, P. Audebert, J. C. Gauthier, J.-P. Geindre, and T. Wittmann, Phys. Rev. E **69**, 026402 (2004).
[19]A. Lévy, T. Ceccotti, P. D'Oliveira, F. Réau, M. Perdrix, F. Quéré, P. Monot, M. Bougeard, H. Lagadec, P. Martin, J.-P. Geindre, and P. Audebert, Opt. Lett. **32**, 310 (2007).
[20]Ch. Ziener, P. S. Foster, E. J. Divall, C. J. Hooker, M. H. R. Hutchinson, A. J. Langley, and D. Neelya, J. Appl. Phys. **93**, 768 (2003).
[21]B. Dromey, S. Kar, M. Zepf, and P. Foster, Rev. Sci. Instrum. **75**, 645 (2004).
[22]Y. Nomura, L. Veisz, K. Schmid, T. Wittmann, J. Wild, and F. Krausz, New J. Phys. **9**, 9 (2007).
[23]J. Liu, C. Wang, B. Liu, B. Shuai, W. Wang, Y. Cai, H. Li, and G. Ni, Phys. Rev. A **73**, 033201 (2006).
[24]D. von der Linde and H. Schüler, J. Opt. Soc. Am. B **13**, 216 (1996).
[25]D. von der Linde, K. Sokolowski-Tinten, and J. Bialkowski, Appl. Surf. Sci. **109–110**, 1 (1997).
[26]F. Brunel, Phys. Rev. Lett. **59**, 52 (1987).
[27]K. Estabrook and W. L. Kruer, Phys. Rev. Lett. **40**, 42 (1978).